

Anisotropic sub-Doppler laser cooling in dysprosium magneto-optical traps

Seo Ho Youn, Mingwu Lu, and Benjamin L. Lev

Department of Physics, University of Illinois at Urbana-Champaign, Urbana, Illinois 61801-3080, USA

(Received 19 July 2010; published 5 October 2010)

Magneto-optical traps (MOTs) of Er and Dy have recently been shown to exhibit populationwide sub-Doppler cooling due to their near degeneracy of excited- and ground-state Landé g factors. We discuss here an additional, unusual intra-MOT sub-Doppler cooling mechanism that appears when the total Dy MOT cooling laser intensity and magnetic quadrupole gradient increase beyond critical values. Specifically, anisotropically sub-Doppler-cooled cores appear, and their orientation with respect to the quadrupole axis flips at a critical ratio of the MOT laser intensity along the quadrupole axis versus that in the plane of symmetry. This phenomenon can be traced to a loss of the velocity-selective resonance at zero velocity in the cooling force along directions in which the atomic polarization is oriented by the quadrupole field. We present data characterizing this anisotropic laser cooling phenomenon and discuss a qualitative model for its origin based on the extraordinarily large Dy magnetic moment and Dy's near degenerate g factors.

DOI: 10.1103/PhysRevA.82.043403

PACS number(s): 37.10.De, 37.10.Gh, 37.10.Vz

I. INTRODUCTION

Ultracold dipolar gases are emerging as an important tool for exploring strongly correlated physics in a system with easily and rapidly tunable parameters. Highly magnetic atoms provide the ability to realize strongly correlated systems in the absence of polarizing fields, which will be important for exploring, for example, quantum liquid crystal physics [1]. Additionally, degenerate fermionic and bosonic dipolar gases are expected to exhibit a wide range of interesting quantum phases and dynamical properties [2]. Dysprosium, the most magnetic laser cooled and trapped gas [3,4], is especially exciting since its $\mu = 10 \mu_B$ magnetic dipole moment—coupled with its large mass and abundance of bosonic and fermionic isotopes—is sufficiently strong to allow wide exploration of ultracold dipolar physics [3–5].

Sub-Doppler cooling [6] in an optical molasses [7] subsequent to MOT capture is a crucial step toward creating degenerate gases in, for example, alkali-metal atomic systems such as Rb and Cs. Sub-Doppler mechanisms fail to cool the majority of atoms [8] inside these MOTs because the ground-state g_g factor is substantially different from the excited state's (for ^{87}Rb , $\Delta g/g_g = 34\%$) [9]; population-wide $\sigma^+ - \sigma^-$ sub-Doppler cooling breaks down in the longitudinal magnetic fields of a typical MOT. Notable exceptions¹ are the highly magnetic lanthanides Er ($7 \mu_B$) and Dy, whose repumper-less MOTs [3,10] operate on optical transitions whose ground- and excited-state g factors are the same to within 0.3% (1.7%) for Er (Dy) [11]. At low MOT beam intensity, both the Er and Dy MOTs exhibit *in situ*, populationwide sub-Doppler cooling [4,12]. The minimum temperatures $>200 \mu\text{K}$ are, however, more than 10 times larger than typical Rb and Cs optical molasses sub-Doppler cooled temperatures, but are similar to sub-Doppler temperatures in the ^{87}Sr MOT [13].

We describe here a sub-Doppler cooling mechanism in the highly magnetic Dy MOT system that we reported in Refs. [3,4]. We expand on these observations with additional

measurements and offer a plausible explanation for this phenomenon based on the theory of velocity-selective resonances (VSRs) in a highly magnetic gas [14–16]. While this mechanism only cools a small fraction of the atoms to $\sim 10 \mu\text{K}$ ultracold temperatures, its existence is an example of novel behavior arising from laser cooling the most magnetic atom.

II. Dy MOT REGIMES

We choose to describe here the Dy MOT system in which all pairs of MOT beams are well aligned in mutual orthogonality and retroreflection.² All data are taken with the experimental apparatus for Dy MOT production described in Ref. [4]. Briefly, a high-temperature oven along with transverse laser cooling produce a collimated atomic beam. A Zeeman slower, operating with 1 W of laser power on the 421-nm cycling transition, decelerates the beam before MOT capture on the 421-nm line (see Fig. 1). No repumper is necessary since the highly magnetic atoms remain confined in the MOT's magnetic quadrupole trap as population decays through metastable states [3,4]. We focus here on the bosonic isotope ^{164}Dy with zero nuclear spin I , but similar results were observed in the fermionic ^{163}Dy MOT ($I = 5/2$).

The Dy MOT can be formed in two classes of operation, striped and stripeless, and the striped MOT can be further classified into three regimes. The stripeless Dy MOT is similar to the Er MOT reported in Ref. [12], in that the majority of atoms are sub-Doppler cooled to $\sim 200 \mu\text{K}$. These MOTs are obtained at low intensity $\bar{I} = I_t/I_s \lesssim 0.17$, where $I_t = I_z + 2I_\rho$ is the total MOT intensity (one beam pair in \hat{z} and two in $\hat{\rho}$) and I_s is the saturation intensity in the MOT; $I_s = 2.7 \times 58 \text{ mW/cm}^2$ [4]. Moreover, the stripeless ^{164}Dy MOT forms at low MOT magnetic quadrupole field $\nabla_z B \lesssim 12 \text{ G/cm}$, where $\nabla_z B \approx 2\nabla_\rho B$ and \hat{z} and $\hat{\rho}$ are the directions along the quadrupole's axis and the plane of symmetry, respectively.

¹The ^{87}Sr system, which has a negligible g_g , also exhibits intra-MOT sub-Doppler cooling [13].

²Boundaries between the striped MOT regimes are blurred with substantial beam misalignment.

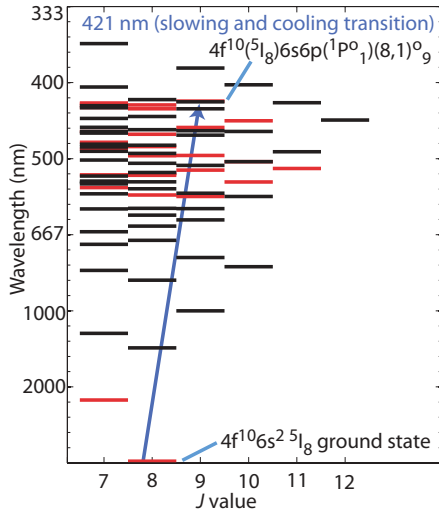


FIG. 1. (Color online) ^{164}Dy energy level structure [11]. The MOT and the Zeeman slower employ the strongest laser cooling transition between the even parity (red) ground state and the odd (black) excited state at 421 nm. For this transition, the g factor of the ground (excited) state is 1.24 (1.22) and the Doppler cooling limit is $T_D^0 = 768 \mu\text{K}$. J is the total electronic angular momentum.

The temperature and density distributions in the three striped MOT regimes differ greatly from the stripeless MOT in time of flight. The temperature distribution is anisotropic at large \bar{I} and $\nabla_z B$, and Fig. 2 shows characteristic time-of-flight expansions of the striped Dy MOT. In these images, MOT beams and the quadrupole field are extinguished at $t_d = 0$, and the *in situ* images are taken at $t_d < 0$. We observe in time of flight a low-population core surrounded by a more populous and hotter outer shell, and we designate the group of outer-shell atoms as the majority whereas we designate

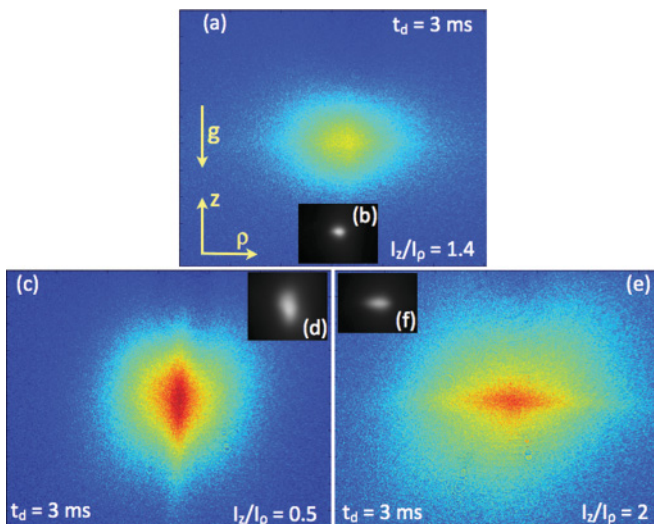


FIG. 2. (Color online) (a, c, e) Time-of-flight expansions and (b, d, f) *in situ* images of the three striped MOT regimes exhibiting anisotropically sub-Doppler cooled cores. (a, b) Symmetric (cross) MOT with $I_z/I_\rho = 1.4$. Notice the faint vertical and horizontal stripes crossing at the MOT center. (c, d) Prolate-striped MOT with $I_z/I_\rho = 0.5$. (e, f) Oblate-striped MOT with $I_z/I_\rho = 2$.

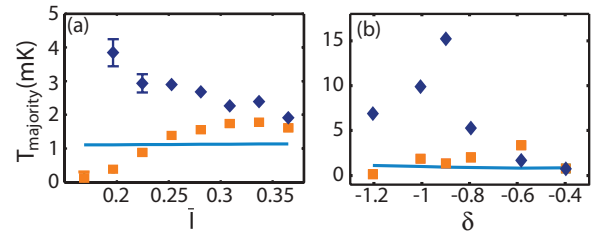


FIG. 3. (Color online) Temperature characterization of the prolate-striped Dy MOT [Fig. 2(c)] versus normalized intensity \bar{I} and detuning δ . The orange squares (blue diamonds) are the T_{majority} along $\hat{\rho}$ (\hat{z}). The light blue curves show the Doppler cooling limit [7] for the MOT parameters: (a) $\delta = -1.2$, $\nabla_z B = 20$ G/cm; (b) $\bar{I} = 0.2$, $\nabla_z B = 20$ G/cm.

the atoms of the inner core as the minority. Parametrically driving the MOT could reveal the minority component's *in situ* size [17].

Typical high-population MOTs are formed with $\bar{I} = 0.2$ and $\delta = \Delta/\Gamma = -1.2$, where Δ is the detuning from the $\Gamma = 2\pi \cdot 32$ MHz, 421-nm transition. These typical MOT parameters correspond to T_D 's of approximately 1 mK. At large MOT intensity, the temperature of the majority component T_{majority} is consistent with T_D , as shown in the $\hat{\rho}$ (orange square) data of Fig. 3 and as discussed in detail in Ref. [4]. The T_{majority} data in $\hat{\rho}$ are derived from the broader of the two Gaussians employed to fit intensity versus ρ [see Fig. 4(b)]. Temperature data for \hat{z} (blue diamond) are derived from single Gaussian fits to intensity versus z [see Fig. 4(c)].

The larger \hat{z} temperature data are a result of the convolution of the Doppler-cooled majority temperatures with the minority velocity distribution along \hat{z} (described in Sec. VI). We note that T_{majority} data in \hat{z} below $\bar{I} \approx 0.17$ are roughly equal to the $\hat{\rho}$ data and are not shown. This low-intensity, sub-Doppler cooled region is also the region in which stripes cease to appear in time-of-flight expansions: In the Dy system, the stripeless regime is the low-intensity limit of the striped regime. We note in the data of Ref. [12] that the sub-Doppler-cooled

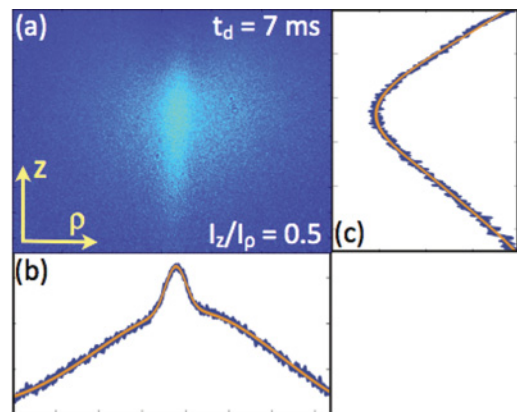


FIG. 4. (Color online) (a) Prolate-striped MOT time-of-flight expansion at $t_d = 7$ ms. (b) Double-Gaussian fit, orange line, along a \hat{z} intensity integration. (c) Intensity integration along $\hat{\rho}$ is consistent with a single Gaussian fit.

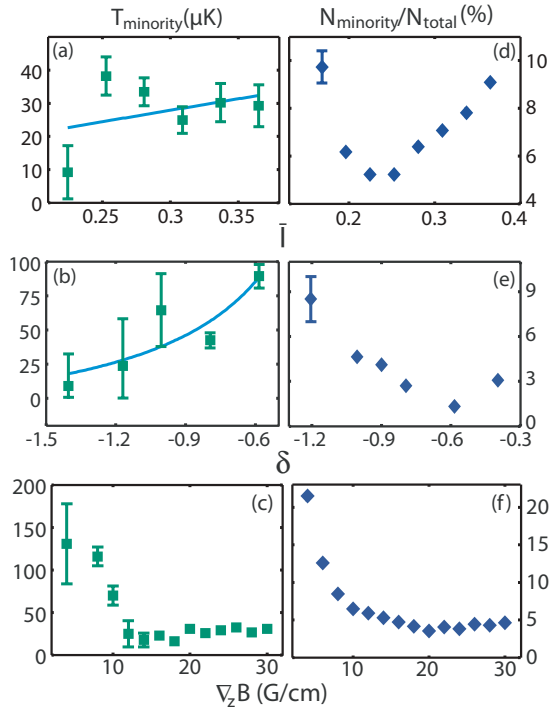


FIG. 5. (Color online) T_{minority} in $\hat{\rho}$ of the prolate-striped MOT $I_z/I_\rho = 0.5$ [Fig. 2(c)]. Blue curves (gray) in (a) and (b) are fits of the data to the sub-Doppler cooling expression, Eq. (1). (d–f) Fractional population of the minority component. (a, d) $\delta = -1.2$, $\nabla_z B = 20$ G/cm; (b, e) $\bar{I} = 0.2$, $\nabla_z B = 20$ G/cm; (c, f) $\bar{I} = 0.2$, $\delta = -1$.

Er MOT, which did not exhibit stripes, was also operated below $\bar{I} = 0.17$.

III. QUANTITATIVE CHARACTERIZATION OF ANISOTROPIC SUB-DOPPLER COOLING

The minority component assumes a prolate, a symmetric (cross), or an oblate shape in time of flight depending on whether the ratio of intensity in the MOT beams I_z/I_ρ is <1.4 , ~ 1.4 , or >1.4 (see Fig. 2). MOT populations are largest in the prolate, $I_z/I_\rho < 1.4$ regime, whose minority component temperature T_{minority} and ratio of minority atoms to total MOT population $N_{\text{minority}}/N_{\text{total}}$ are shown in Fig. 5.³

T_{minority} and N_{minority} are extracted from a double-Gaussian fit to time-of-flight data such as that presented in Fig. 4. The temperature of the minority component is anisotropic, leading to the vertical stripe structure in Figs. 2(c) and 4(a). The temperature in \hat{z} is hotter than that of the majority atoms [see the \hat{z} (blue diamond) data of Fig. 3], while the temperature in $\hat{\rho}$ is sub-Doppler cooled to temperatures as low as 10 μK , a factor of 10 less than the sub-Doppler temperatures observed in the stripeless regime. The $\hat{\rho}$ temperature of the minority component in the prolate MOT is well described by a

³Careful characterization of minority population and temperature for MOTs with $I_z/I_\rho > 1$ was inhibited by increased MOT population instability in these regimes.

one-dimensional (1D) characteristic sub-Doppler scaling law [8,13]:

$$T_\rho = T_0 + C_{\sigma^+\sigma^-} \frac{\hbar\Gamma\bar{I}}{2k_B|\delta|}, \quad (1)$$

where $[C_{\sigma^+\sigma^-}] = [0.1(0.09), 0.55(0.20)]$ in Figs. 5(a) and 5(b), respectively. These values of $[C_{\sigma^+\sigma^-}]$ are consistent with those of the Er MOT [12], but smaller than in the ^{87}Sr MOT [13]. However, T_0 is <10 μK in both fits and is about ten times lower than in the Er, Sr, and stripeless Dy MOTs. This two-dimensional (2D), anisotropic sub-Doppler cooling—in the case of the oblate-striped MOT, 1D⁴—is a cooling mechanism much more effective than the one found in the stripeless sub-Doppler-cooled Er and Dy MOTs.

IV. TRANSITION BETWEEN PROLATE AND OBLATE STRIPED MOTS

We explore the transition between the prolate- and oblate-striped Dy MOT in Fig. 6. As the MOT's I_z/I_ρ ratio is tuned from 0.5 to 2, we note the occurrence—defined by visibility of the double-Gaussian structure above the image noise—of stripes in a series of ten realizations. The fraction of these images exhibiting a stripe structure is noted in Fig. 6. Below $I_z/I_\rho = 1$, the prolate stripe is always observed, while the oblate stripe is always observed above $I_z/I_\rho = 2$. There is a smooth transition between the regimes in which successive MOT realizations may exhibit either a prolate stripe or an oblate stripe, and we can offer no explanation for either the smoothness of the transitions or their slight asymmetry.

Between these two regimes there is a third: We most often observe a spherically symmetric minority component in the range of I_z/I_ρ from 1.3 to 1.5. This is the regime of the power balanced and aligned MOT discussed in Ref. [3] and is less populous, though more dense, than the prolate regime. A prolate-oblate cross is observed [see Fig. 2(a)] in the region around the critical ratio $I_r^c = I_z/I_\rho = 1.4$, though

⁴We observe, by imaging in the ρ plane, that the oblate stripe is indeed azimuthally symmetric.

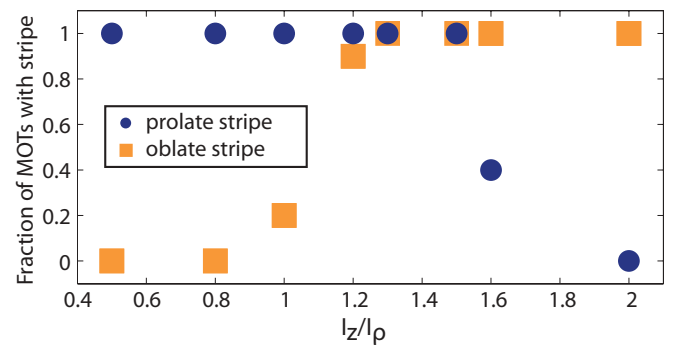


FIG. 6. (Color online) Visibility of stripe regimes—prolate, symmetric (cross), and oblate—versus the ratio of MOT beam power I_z/I_ρ . Data are taken for $\bar{I} = 0.22(0.01)$, $\delta = -1$, and $\nabla_z B = 20$ G/cm. All stripes vanish below $\bar{I}_c = 0.17$. Each point is the average of 10 MOT realizations with $t_d = 6.5$ ms.

not reproducibly, and the spherically symmetric core is more prevalent.

No stripes are observed below the critical intensity $\bar{I}_c < 0.17$, which coincides with the appearance of the majority component (populationwide) sub-Doppler cooling [see Fig. 3]. The prolate stripe is observed to vanish below a critical $\nabla_z B_c \approx 12$ G/cm, as shown in Fig. 5(c). The minority component temperature and stripe population fraction rise below $\nabla_z B_c$ —which may be interpreted as a blending of the minority and majority components—until the MOT is firmly in the stripeless, isotropically sub-Doppler-cooled regime.

V. VELOCITY SELECTIVE RESONANCE PICTURE OF ANISOTROPIC SUB-DOPPLER COOLING

This section presents a qualitative explanation of the anisotropic sub-Doppler cooling mechanism. Two properties of Dy are crucial to this explication: its large magnetic moment and the near equal ground-state and excited-state g factors ($\Delta g \approx 0$) of the cooling transition. The latter is important for the following reason. In standard $\sigma^+ - \sigma^-$ sub-Doppler cooling, the linear optical polarization serves as the quantization axis since the optical pumping rate γ_p is typically greater than the Larmor precession rate $\omega_L = \mu \nabla B r / \hbar$, where r is the distance of the atom from the magnetic quadrupole's center. In low magnetic fields, ground-state population imbalance due to nonadiabatic following of the quantization axis induces the differential scattering of σ light, which then leads to sub-Doppler cooling to zero mean velocity [6,7]. However, in large longitudinal magnetic fields, a nonzero Δg results in an “unlocking” of the Doppler and sub-Doppler cooling mechanisms, and sample temperatures rise to the Doppler cooling limit. (Hence the failure of populationwide sub-Doppler cooling in, e.g., Rb MOTs and the need for field nulling to the mG level when sub-Doppler cooling in Rb optical molasses.) By contrast, Er and Dy MOTs remain sub-Doppler cooled [4,12] despite the large intra-MOT magnetic fields because $\Delta g \approx 0$ in both. This explains the existence of intra-MOT sub-Doppler cooling in Er and Dy, but not the origin of the anisotropic regime.

The anisotropic sub-Doppler cooling mechanism may be qualitatively understood in the VSR picture of 1D sub-Doppler cooling [14] when augmented to account for large magnetic fields or, equivalently, large magnetic moments.⁵ In this picture, most types of sub-Doppler cooling may be understood as arising from the momentum transfer by a coherent two-photon process between ground-state sublevels (labeled by m) [14]. These coherent Raman transitions can occur when the difference in Doppler-shifted frequencies of counterpropagating light beams seen by an atom equals the Zeeman shift between levels separated by $\Delta m = n$.

⁵A review of such a treatment is beyond the scope of the current work. However, Refs. [15,16] provide detailed analytical and numerical calculations of the force and diffusion felt by atoms in various relative orientations of (a large) magnetic field and $\sigma^+ - \sigma^-$ light; see Figs. 4 and 5 and Table 1 of Ref. [15] and Fig. 4 of Ref. [16] for force versus velocity plots and additional details of the VSR cases invoked in Sec. V.

Specifically, VSRs occur when $\delta \mathbf{k} \cdot \mathbf{v} = n \mu_B B$, where \mathbf{v} is the atom's velocity and $\delta \mathbf{k} = 2\mathbf{k}$ is the difference in the wave vectors of the $\sigma^+ - \sigma^-$ light. The allowed n 's depend on the relative orientation of optical and magnetic field vectors, and it is this selection rule that is the origin of the anisotropic sub-Doppler cooling in the large field (large magnetic moment) regime.

To see how this selection rule leads to anisotropic cooling, we first note that the atoms' polarization aligns along the local magnetic field in the presence of a large magnetic field (or large moment), defined as $\gamma_p \ll \omega_L \ll \Gamma$; in this large Zeeman energy regime, the magnetic field now serves as the quantization axis, not the optical polarization [15]. Now we examine the case in which the magnetic field is aligned parallel to the \mathbf{k} 's of a pair of $\sigma^+ - \sigma^-$ beams. Along the spatial directions defined by the \mathbf{k} 's of the cooling light, the zero-mean-velocity VSR in the cooling force disappears ($n \neq 0$) even though finite-velocity VSRs remain ($n \geq 2$ are allowed). This is because there is no component of the polarization along the magnetic field (azimuthal symmetry about \mathbf{k} is preserved), and thus no π transitions are allowed, which are necessary for $n = 0$ and $n = 1$ VSRs. In this case, sub-Doppler cooling to zero velocity along directions close to \mathbf{k} is not possible when $\mathbf{B} \parallel \mathbf{k}$.

However, not all sub-Doppler cooling is suppressed. A zero-velocity VSR remains in the cooling force along directions in which the local magnetic field is perpendicular to the cooling light's \mathbf{k} 's (for $\mathbf{B} \perp \mathbf{k}$ all n are allowed). This spatial modulation of allowable VSRs (n 's) is the origin of the anisotropic nature of the sub-Doppler cooling observed in the highly magnetic Dy system.

In summary, $\sigma^+ - \sigma^-$ sub-Doppler cooling is preserved (fails) along directions perpendicular (parallel) to the local magnetic field in systems with large magnetic fields or large magnetic moments. Figure 7(b) illustrates this idea for the prolate-striped MOT: sub-Doppler cooling occurs along $\hat{\rho}$ due to the green \mathbf{k}_ρ $\sigma^+ - \sigma^-$ beams, but not along \hat{z} due to atomic polarization orientation parallel to the magnetic field. The red \mathbf{k}_z $\sigma^+ - \sigma^-$ beams only induce VSRs with nonzero velocity (e.g., $n \geq 2$) in the cooling force, and these beams cause the atoms to accelerate along \hat{z} due to the magnetic quadrupole field gradient. The analogous mechanism holds for the oblate MOT when the magnetic field (quantization axis) is along $\hat{\rho}$ instead.

Prolate and oblate stripes oriented with respect to the quadrupole axis dominate because the only regions wherein the magnetic field is parallel to the \mathbf{k} vectors are those in

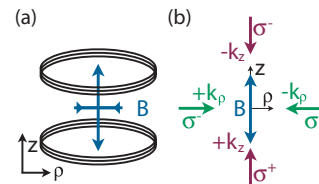


FIG. 7. (Color online) (a) Orientation of the MOT's magnetic quadrupole field. (b) Illustration of the anisotropic cooling in the prolate MOT including the MOT magnetic (B) field orientation, cooling-beam wave vectors \mathbf{k} , and polarizations σ^\pm near the z axis.

the plane or along the axis of symmetry of the quadrupole field. The regions' small relative volume is the origin of $N_{\text{minority}}/N_{\text{total}} < 10\%$. We note that this $\sigma^+-\sigma^-$ mechanism is distinct from $\sigma^+-\sigma^+$ magnetically induced laser cooling [7].

VI. ANISOTROPIC SUB-DOPPLER COOLING IN THE Dy SYSTEM

Although this description does not predict the prolate-to-oblate transition, our quantitative measurements in the prolate regime are consistent with this picture. Specifically, when $I_z/I_\rho < I_r^c$, $\bar{I} > \bar{I}_c$, and $\nabla_z B > \nabla_z B_c$ such that a prolate-stripped MOT forms, we observe higher-than-Doppler-limited temperatures along the \hat{z} direction, which lies parallel to the local magnetic field (Fig. 3). As mentioned in the previous section, this is because along the $\mathbf{B} \parallel k$ direction the atoms accelerate as they move away from the trap center due to ever increasing magnetic fields and VSR velocities. An estimate of these resonant velocities—based on $v = \omega_z/k$ [14] in the 20 G/cm gradient field along \hat{z} —are $\geq T_D$ and are thus consistent with the absence of any sub-Doppler cooling mechanism along this direction. Specifically, outside a core of radius 30 μm —roughly the zone outside which anisotropic sub-Doppler cooling occurs (see below)—the velocities are > 0.35 m/s, resulting in 1D temperatures of > 2.5 mK. Such temperatures are larger than the $T_D \approx 1$ mK limit for the typical Dy MOT parameters [see blue (gray) curves in Fig. 3].

Anisotropic sub-Doppler cooling is possible for the Dy MOT on the 421-nm, $\Delta g \approx 0$ transition because $\gamma_p \ll \omega_L \ll \Gamma$ is satisfied throughout the majority of the Dy MOT's quadrupole field. Specifically, Dy's optical pumping rate

$\gamma_p \approx \bar{I}\Gamma/(1 + \bar{I} + 4\delta^2)$ is approximately equal to the light shift frequency, and the inequality is satisfied with the range of values $[\gamma_p, \omega_L, \Gamma] = 2\pi[0.8, 1 - 28, 32]$ MHz present in a typical Dy MOT with $\nabla B = 20$ G/cm and $0.04 < r < 1$ mm. In addition, $\gamma_p/\omega_L < 1$ for $\nabla B > 10$ G/cm, which is close to the measured critical value $\nabla_z B_c/2 = \nabla_\rho B_c \approx 12$ G/cm. We do not have a simple estimate for $\bar{I}_c = 0.17$ and $I_r^c = 1.4$, but we expect that 2D numerical simulations of the Dy MOT could explicate the origin of these specific values as well as the underlying mechanism behind the stripe orientation transitions.

VII. CONCLUSION

In conclusion, we note the possibility that other highly magnetic lanthanides could exhibit anisotropic sub-Doppler cooling for large enough cooling beam intensity and field gradient: This novel cooling mechanism should be observable in Er MOTs when larger MOT beam intensities are employed. The highly magnetic atom Ho (9 μB , $\Delta g/g_g = 1.7\%$)—of interest for quantum-information processing [18]—would likely exhibit anisotropic sub-Doppler cooling as well, if it were proven amenable to repumperless magneto-optical trapping.

ACKNOWLEDGMENTS

We thank J. V. Porto and W. D. Phillips for discussions, J. Ye for a critical reading of the manuscript, and N. Burdick for technical assistance. We acknowledge support from the NSF (PHY08-47469), the AFOSR (FA9550-09-1-0079), and the Army Research Office MURI Grant W911NF0910406.

-
- [1] B. M. Fregoso, K. Sun, E. Fradkin, and B. L. Lev, *New J. Phys.* **11**, 103003 (2009); B. M. Fregoso and E. Fradkin, *Phys. Rev. Lett.* **103**, 205301 (2009); *Phys. Rev. B* **81**, 214443 (2010).
 - [2] T. Lahaye, C. Menotti, L. Santos, M. Lewenstein, and T. Pfau, *Rep. Prog. Phys.* **72**, 126401 (2009); T. Sogo, L. He, T. Miyakawa, S. Yi, H. Lu, and H. Pu, *New J. Phys.* **11**, 055017 (2009); S. Ronen and J. L. Bohn, *Phys. Rev. A* **81**, 033601 (2010); J. A. M. Huhtamäki, M. Takahashi, T. P. Simula, T. Mizushima, and K. Machida, *ibid.* **81**, 063623 (2010).
 - [3] M. Lu, S.-H. Youn, and B. L. Lev, *Phys. Rev. Lett.* **104**, 063001 (2010).
 - [4] S.-H. Youn, M. Lu, U. Ray, and B. L. Lev (2010), e-print arXiv:1007.1480.
 - [5] S. Yi, T. Li, and C. P. Sun, *Phys. Rev. Lett.* **98**, 260405 (2007).
 - [6] J. Dalibard and C. Cohen-Tannoudji, *J. Opt. Soc. Am. B* **6**, 2023 (1989); P. Ungar, D. S. Weiss, E. Riis, and S. Chu, *ibid.* **6**, 2058 (1989).
 - [7] H. J. Metcalf and P. van der Straten, *Laser Cooling and Trapping* (Springer-Verlag, New York, 1999).
 - [8] M. Drewsen, P. Laurent, A. Nadir, G. Santarelli, A. Clairon, Y. Castin, D. Grison, and C. Salomon, *Appl. Phys. B* **59**, 283 (1994).
 - [9] M. Walhout, J. Dalibard, S. L. Rolston, and W. D. Phillips, *J. Opt. Soc. Am. B* **9**, 1997 (1992); J. Werner, H. Wallis, and W. Ertmer, *Opt. Commun.* **94**, 525 (1992).
 - [10] J. J. McClelland and J. L. Hanssen, *Phys. Rev. Lett.* **96**, 143005 (2006).
 - [11] W. C. Martin, R. Zalubas, and L. Hagan, *Atomic Energy Levels—The Rare Earth Elements* (NSRDS-NBS, Washington, DC, 1978), Vol. 60.
 - [12] A. J. Berglund, S. A. Lee, and J. J. McClelland, *Phys. Rev. A* **76**, 053418 (2007).
 - [13] X. Xu, T. H. Loftus, J. W. Dunn, C. H. Greene, J. L. Hall, A. Gallagher, and J. Ye, *Phys. Rev. Lett.* **90**, 193002 (2003).
 - [14] S.-Q. Shang, B. Sheehy, H. Metcalf, P. van der Straten, and G. Nienhuis, *Phys. Rev. Lett.* **67**, 1094 (1991).
 - [15] P. van der Straten, S.-Q. Shang, B. Sheehy, H. Metcalf, and G. Nienhuis, *Phys. Rev. A* **47**, 4160 (1993).
 - [16] S. Chang, T.-Y. Kwon, H.-S. Lee, and V. G. Minogin, *Phys. Rev. A* **66**, 043404 (2002).
 - [17] K. Kim, H.-R. Noh, H.-J. Ha, and W. Jhe, *Phys. Rev. A* **69**, 033406 (2004).
 - [18] M. Saffman and K. Mølmer, *Phys. Rev. A* **78**, 012336 (2008).